

Invited Perspective

Site-specific variation in the activity of COX-2 alters the pattern of wound healing in the tail and limb of northern house gecko by differentially regulating the expression of local inflammatory mediators

Kashmira Khaire, Urja Verma, Pranav Buch, Sonam Patel, Isha Ranadive, Suresh Balakrishnan *

Department of Zoology, Faculty of Science, The Maharaja Sayajirao University of Baroda, Vadodra, 390001, Gujarat, India



ARTICLE INFO

Keywords:

Lizard tail
Lizard limb
Wound healing
COX-2
Inflammation

ABSTRACT

The role of COX-2 induced PGE₂ in the site-specific regulation of inflammatory mediators that facilitate disparate wound healing in the tail and limb of a lizard was studied by analysing their levels during various stages of healing. The activity of COX-2 and concentration of PGE₂ surged during the early healing phase of tail along with the parallel rise in EP4 receptor. PGE₂-EP4 interaction is corelated to early resolution (by 3 dpa) of inflammation by rising the antiinflammatory mediator IL-10. This likely causes reduction in proinflammatory mediators viz., iNOS, TNF- α , IL-6, IL-17 and IL-22. Conversely, in the limb, COX-2 derived PGE₂ likely causes rise in inflammation through EP2 receptor-based signalling, as all the proinflammatory mediators stay elevated through the course of healing (till 9 dpa), while expression of IL-10 is reduced. This study brings to light the novel roles of IL-17 and IL-22 in programming wound healing. As IL-17 reduces in tail, IL-22 behaves in reparative way, causing conducive environment for scar-free wound healing. On the contrary, synergic elevation of both IL-17 and IL-22 form a micro-niche suitable for scarred wound healing in limb, thus obliterating its regenerative potential.

1. Introduction

A near perfect wound healing potential is an accreditation achieved by a few of the vertebrates, which helps them to repair and rejuvenate the lost tissues and organs, thereby increasing their chances of survival (Agata et al., 2007). In the case of regeneration-compatible organisms like salamanders, injury to tissue leads to scar-free wound healing that in turn facilitates complete restoration of the lost structure (Suzuki et al., 2006; Vervoort, 2011). However, in higher vertebrates, including humans, tissue injury is followed by a wound healing pattern, which results in a permanent scar at the site of injury with no or little regenerative response (Bely, 2010). The current study is an attempt to explore the reasons behind this disparity of wound healing routes while keeping the inflammation as a focal point. Being the preliminary response to any physical assault, inflammation is expected to play a crucial role in deciding the path of wound healing.

Numerous animal models are being studied globally to unravel the details of scar-free wound healing and resultant regeneration. One such model organism is northern house gecko, *Hemidactylus flaviviridis*, which

can selectively regenerate the lost tail while the other appendages (limbs) follow scarring upon amputation (Buch et al., 2017, 2018; Ranadive et al., 2018). Investigating this intriguing yet less studied model will lead to a better insight into the events leading to the scar-free wound healing, a prerequisite for subsequent regeneration. Additionally, any mechanistic details thus gained can help in understanding the causes of limited restorations, as observed in humans. The wound healing however is synchronized by many parallel processes, which either boost or hinder its proceedings. Of all these events, the local inflammation could be an imperative factor since it can regulate the course of healing and behave as a double-edged sword due to its crucial role in orchestrating regeneration, along with the perturbing interference observed, under its prolonged stay (Mescher et al., 2013). Therefore, this study was designed to highlight the possible role of inflammation in organising differential wound healing observed in the lizard *H. flaviviridis*.

The intricate event of inflammation is attributed to the cumulative function of different inflammatory mediators, which either boost its stay or help in resolving it (Prisk and Huard, 2003; Peranteau et al., 2008;

Abbreviations: dpa, Days post-amputation; COX, Cyclooxygenase; PGE₂, Prostaglandin E₂; PGD₂, Prostaglandin D₂; EP1-4, Prostaglandin E receptor family; IL, Interleukins; iNOS, inducible Nitric Oxide synthase; TNF- α , Tumour Necrosis Factor α .

* Corresponding author.

E-mail address: b.suresh-zoo@msubaroda.ac.in (S. Balakrishnan).

<https://doi.org/10.1016/j.zool.2021.125947>

Received 10 February 2021; Received in revised form 29 May 2021; Accepted 23 June 2021

Available online 25 June 2021

0944-2006/© 2021 Elsevier GmbH. All rights reserved.

Korbecki et al., 2014; Gilbert et al., 2015). These humoral players might develop a micro niche at the site of injury to either lead to a scar-free healing or non-regenerative scar formation (Chamberlain et al., 2013; Karin and Clevers, 2016). In an effort to unearth the basic mechanisms, after a series of preliminary screening, the regulators of inflammation like cyclooxygenase-2 (COX-2), prostaglandin E₂ (PGE₂), prostaglandin E receptor (EP2 and EP4) followed by inflammatory mediators, namely iNOS, TNF- α , IL-6, IL-10, IL-17, and IL-22, which function in coordination with COX-2, were considered for this study. The specific choice of COX-2 as a mediator of interest was made in the light of previous study from our lab, which highlights its role in achieving epithelialisation and proliferation in the regenerating tail of *H. flaviviridis* via Wnt/ β -Catenin pathway (Buch et al., 2017). In few other studies, role of COX-2 derived PGE₂ has been proven in initiation and progression of regeneration in lizard tail (Sharma and Suresh, 2008; Buch et al., 2018). In the present report, 'COX-2' has been used, uniformly, instead of the gene name-PTGS-2, to avoid confusion.

This work, therefore, focused on the role of inflammatory mediators in governing the pattern of wound healing, through its pivotal participation in the differential regulation of inflammation in two healing tissues, viz., the tail and limb. The detailed architecture of the healing tail and limb have been elaborately reported by Alibardi (2014) and Vitulo et al. (2017), using immunohistochemistry. The novel aspect observed in this study is the appendage-specific action of inflammatory mediators, which leads to its early resolution or prolonged stay in the healing microenvironment that further causes either a scar-free wound healing as a forerunner of regenerative outgrowth in tail or forms a permanent scar tissue in the limb.

2. Materials and Methods

2.1. Procurement of animals and maintenance

Hemidactylus flaviviridis (northern house gecko), both male and female, were caught from a nearby locality and caged in wooden chambers. Housing conditions were maintained as reported by Buch et al. (2017). Briefly, the animals selected for studies weighed around 10-12 g and were maintained at 34 \pm 2 °C with light to dark cycle of 12:12 hours. The experimental protocol (MSU-Z/IAEC/15-2017) was approved by the institutional animal ethics committee (IAEC) and all the experiments were performed as per the guidelines of CPCSEA, India.

2.2. Animal grouping and experimental design

For investigating the molecular events of inflammation in the appendages, the animals were randomly categorised into two main groups, namely tail and limb. These groups were further divided in various sub-groups based on the stage of the healing process to be targeted. For tail, 0, 1, 2, 3, and 4 dpa (days post-amputation) and for limb, 0, 3, 6 and 9 dpa were considered for the study, as these highlight the haemostasis, granulation along with the increased inflammation, culminating in scab formation, followed by appearance of wound epithelium. Ranadive et al. (2018) have reported the distinct time points for attaining the above-mentioned milestones that determine a path of repair in both limb and tail. The same time points are considered here for this investigation. For every experiment, six lizards were used in each sub-group, viz., 0, 1, 2, 3, 4 dpa for Tail and 0, 3, 6 and 9 dpa for limb group, while three technical replicates were performed using pooled samples of six subjects. In the members of tail group, tail was forced to autotomise and the tissue was collected at the predetermined time points to further check the expression status of various inflammatory mediators. Autotomy causes the release of tail, from the fracture plane, where pressure is applied. This end was then observed daily for the specific changes and the segment was collected by applying pressure on the preceding fracture plane for further processing. Concurrently, for the subjects of limb group, their right forelimbs were surgically amputated at the humerus

under hypothermia as described previously by Ranadive et al. (2018), wherein the ice pack was placed on the appendage and the animal was placed on a precooled tile. Tissue was then collected at particular time windows to proceed with the analysis. Around 3 mm of tissue chunk was harvested from the pre-amputated limb, to carry out various analyses as detailed in the following section.

2.3. COX activity assay

Tissues were collected from both the groups at all the above-mentioned time points in 0.1 M Tris-EDTA buffer and 10% tissue homogenate was further used for a spectrophotometric COX assay, following the manufacturer's protocol (Cayman Chemical Co, USA; ID: 760151). The specific activity was calculated in nmol/min/100 g tissue weight. The method deployed in this assay utilised the peroxidase activity of COX, wherein the appearance of the oxidised form of N,N,N',N'-tetramethyl-p-phenylenediamine (TMPD) was measured at 590 nm. TMPD was provided as a ready to use substrate in the kit, while sample prepared from the isolated tissues acted as the enzyme cocktail.

2.4. PGE₂ estimation

Tissue samples were collected from all the subgroups and homogenised in double-distilled water (1 g/4 ml). 15% of v/v methanol was added to this homogenate, and the prostanoids present in it were allowed to be dissolved in the added alcohol for 1 hour. These homogenates were then centrifuged at 4 °C and 2000g for 5 min. The supernatant was collected for the estimation assay of PGE₂ following the manufacturer's protocol (R&D Lab Systems, USA; ID: KGE004B). Herein, the PGE₂ present in the sample competes with the horseradish peroxidase (HRP)-labelled PGE₂ in a sequential competitive binding immunoassay. The colour developed due to the competitive enzyme activity is measured at 450 nm. The estimated levels of PGE₂ were calculated in pg/ml.

2.5. Immunohistochemistry

Freshly collected tissue samples were processed in cryostat-microtome to obtain longitudinal cryo-sections of 8-10 μ m thickness. These were then fixed in chilled acetone for 15-20 min, followed by which, the sections were subjected to rehydration with PBS-T (Phosphate buffered saline + 0.25% Tween-20) and blocked at room temperature for half an hour, with 0.5% bovine serum albumin in PBS (PBS-BSA) (GeNei, Merck, USA), followed by incubation with anti-COX-2 IgG rabbit (0.5 μ g/ml, Sigma-Aldrich, USA). Further, the sections were washed thrice for 15 min. each, with the PBS-T. These sections were then subjected to FITC-conjugated secondary antibody (0.1 μ g/ml, Sigma-Aldrich, USA). Three subsequent buffer washes of 15 min. each and then these sections were used to observe the distribution pattern of COX-2 in different compartments of the tissue. In order to observe the tissue architecture in these sections, DAPI was used to counterstain each one of these, which were then observed under a fluorescent microscope (Leica DM2500, Germany). The representative images were captured using the digital camera (Leica, EC3, Germany), mounted on the microscope.

2.6. Western blot

Samples from all sub-groups of tail and limb groups were collected in lysis buffer [50 mM Tris-HCl (pH 7.5), 200 mM NaCl, 10 mM CaCl₂ and 1% triton-X 100] and were processed at 10,000 g for 10 min. Total protein was estimated by assaying 10% homogenate, using Bradford's method (Bradford, 1976). Further, equal amount of the protein extract was allowed to electrophorese on 12% gel of SDS-PAGE at 100 volts. The components of the gel were transferred on PVDF membrane via semi-dry western blot transfer, at 100 mA for 25 min. This membrane was used to develop immunoblots using specific antibodies against the

inflammatory mediators of interest. The primary antibodies used were, anti- β -actin IgG mouse (0.01 μ g/ml, Santa Cruz Biotechnology, USA), used here as loading control, anti-COX-2 IgG rabbit (0.1 μ g/ml, Sigma-Aldrich, USA), anti-EP2 IgG rabbit (0.1 μ g/ml, Sigma-Aldrich USA), anti-EP4 IgG rabbit (0.1 μ g/ml, Sigma-Aldrich, USA), anti-TNF- α IgG mouse (0.1 μ g/ml, Sigma-Aldrich, USA), anti-IL-6 IgG mouse (0.5 μ g/ml, DSHB, USA), anti-iNOS IgG rabbit (0.1 μ g/ml, Santa Cruz Biotechnology, USA), anti-IL-10 IgG rabbit (0.1 μ g/ml, Santa Cruz Biotechnology, USA), anti-IL-17 IgG rabbit (0.1 μ g/ml, Santa Cruz Biotechnology, USA), anti-IL-22 IgG rabbit (0.1 μ g/ml, Santa Cruz Biotechnology, USA). Host-specific biotinylated secondary antibodies were used for developing the blots, namely anti-rabbit IgG and anti-mouse IgG, developed in goat, procured from Sigma-Aldrich, USA, (1:500). The blots were developed using Streptavidin conjugated ALP as an enzyme, and BCIP-NBT as substrate (Sigma-Aldrich, USA). The primary antibodies raised against the respective antigens in the rabbit and mouse, were used for IHC and Western blot, considering the stringently conserved genetic sequences of these molecules across all the classes of vertebrates (Kaiser et al., 2004; Murphy and Thompson, 2011). Also, the previous work from the lab establishes the cross reactivity of these antibodies in *H. flaviviridis* (Buch et al., 2017, 2018; Ranadive et al., 2018).

2.7. Quantitative real-time PCR

Total RNA was isolated as per the manufacturer's guidelines, from all the tissue samples of both the groups, which were homogenised in TRIzol reagent (Applied Biosystems, USA). 1 μ g of the total RNA was used then to synthesise the cDNA using one-step cDNA synthesis kit (Applied Biosystems, USA). Gene expression of COX-2 and other selected inflammatory mediators was checked using the PCR reaction performed in LightCycler 96 (Roche Diagnostics, Switzerland), using specific primers designed through Primer-Blast tool of NCBI. Primers designed for different macromolecules are mentioned in Table 1.

For the analysis, 18srRNA was used as housekeeping control. Quantitative real-time PCR was performed with the following program: 100 s at 95 °C followed by 40 cycles of 10 s at 95 °C, 30 s at 60 °C, and 30 s at 72 °C. Fold change was calculated using method developed by Livak and Schmittgen (2001) using corresponding group's (limb's or tail's) 0 dpa (resting stage) Δ Cq values, for all the three technical replicates.

2.8. Statistical analyses and grayscale analysis of images

All the quantitative variables are presented as the Mean \pm SEM. Difference between the sample means was computed by one-way analysis of variance (ANOVA), followed by Bonferroni post-hoc test. *p* values \leq 0.05 were considered as significant. Statistical analyses were performed using GraphPad Prism 7.00 (San Diego, USA). Immunohistochemical and western blot images were analysed using ImageJ software (NIH, USA).

Table 1

List of primers used for qRT-PCR analysis.

Gene	Forward (sequence 5'-3')	Reverse (sequence 5'-3')	NCBI ref. Id	Product length
COX-2	ACGTCTTACATCACGATCCC	GGAGAAGGCTTCCCAGCTTTT	NM_001167718.1	86
EP2	AGTTCAGCCAGAGCGAGAAC	AAGACCCAGGGGTGCGATGAT	NM_001083365.1	85
EP4	CATTCTCTGGTGGTCCGTG	GCTTGCAGGTGAGGGTTTGT	NM_001081503.1	87
iNOS	AACATGCTCCTTGAGGTGGG	CAGCTCGGTCTTCCACAAT	NM_204961.1	184
TNF- α	GGGTGTTCCGGTGTGATTT	TCTCACTGCATCGGCTTTGT	NM_001024447.1	171
IL-10	AAGGAGACGTCGAGAAGATGG	TGATGAAGATGTCGAACCTCCC	NM_001004414.2	70
IL-6	TATCTATGAAGCCGCTCCG	CCATCCACCAACATTCGCG	XM_015281283.2	84
IL-17	ACAGGAGATCCTCGTCTCC	CCTTTAAGCCTGGTGTGGA	NM_204460.1	124
IL-22	AAGCGCTGAGTGTGTAAC	CTTTTGGAGGTAGGGGGCTG	NM_001199614.1	150
18srRNA	GGCCGTCTTCTAGTTGGTGA	TCAATCTCGGGTGAAC	NR_003278.3	144

3. Results

3.1. Temporal variation in the activity of COX-2 in the healing tail and limb

COX activity at various stages of scar-free and scarred wound healing were compared in tail (Fig. 1A) and limb (Fig. 1B), respectively. In the tail, the activity of COX-2 showed significant increase at all the wound healing stages of tail, when compared to 0 dpa (Fig. 1A). Similarly, in limb, COX-2 levels increased significantly at 3 dpa, 6 dpa and 9 dpa when compared to 0 dpa (Fig. 1B). Since the COX-2 activity levels were found to be high in both the appendages during their respective healing stages, a major mediator of inflammation downstream of COX-2, which controls the resultant modulations, namely PGE₂ (Prisk and Huard, 2003; Verma et al., 2021; Parmar et al., 2021) was targeted.

3.2. PGE₂ level in the healing appendages

Prostaglandin E₂ is a pivotal contributor to inflammation, synthesis of which is initiated by the injury-induced activation of the enzyme COX-2 (Korbecki et al., 2014). Levels of PGE₂ were analysed at the selected time windows in both tail and limb. An increase in PGE₂ level was observed in tail tissue from 1 dpa till 4 dpa when compared to the resting stage (Fig. 1C). On the other hand, in limb, a downward trend was observed in the level of PGE₂ starting from 3 dpa till 9 dpa, all significantly lower as compared to 0 dpa (Fig. 1D). The readable observation was the well-pronounced reduction observed in the PGE₂ level in limb as opposed to tail.

3.3. Distribution pattern of COX-2 in the healing appendages

COX-2 was localised in the tissues collected at destined time points from both the appendages and the subsequent microscopic analysis vividly portrayed the temporal changes in its site of expression. In tail tissue, initially at 0 dpa, a faint expression of COX-2 at the site of autotomy was observed (Fig. 2A). Although, in the following stages of wound healing in tail, COX-2 was found to be localised differentially. COX-2 was localised near spinal cord at 1 dpa in tail tissue (Fig. 2B) whereas its expression was observed in the intermediate region between epidermis and spinal cord at 2 dpa (Fig. 2C). In 4 dpa tissue, COX-2 was seen just under the epithelial ectoderm of tail (Fig. 2D). In case of limb, visible expression of COX-2 in the tissue section, at the site of amputation in 0 dpa stage was observed (Fig. 2E). At 3 dpa, COX-2 was localised over the injured surface of humerus immediately beneath the clot (Fig. 2F). At 6 dpa, COX-2 was localised in the chondrocytes covering the humerus bone as well as in the newly formed epithelial layer (Fig. 2G). A remarkable difference was observed in the site of COX-2 expression in both tissues (tail and limb), wherein the area of its localisation changed temporally. For instance, COX-2 localisation peculiarly shifted from the proximal region of progressive epithelium covering the amputated limb in 6 dpa (Fig. 2G) to closer to the dermal layer by 9 dpa, where the persistent scar is formed (Fig. 2H). The schematic representation is

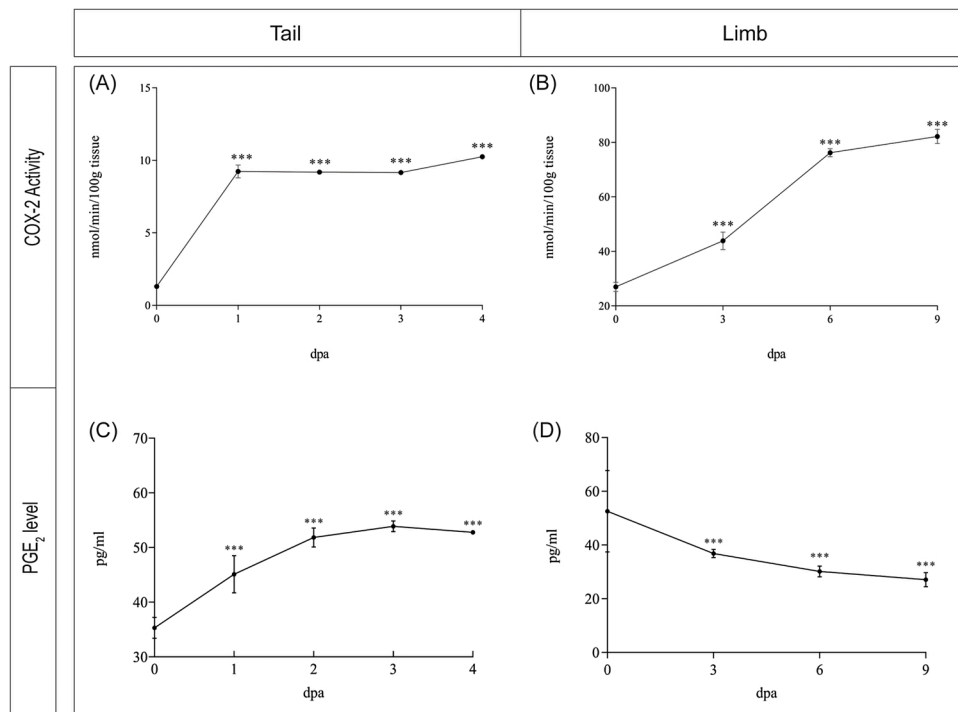


Fig. 1. Enzyme assays: (A) COX-2 activity in healing tail. (B) COX-2 activity in healing limb. (C) PGE₂ level in healing tail. (D) PGE₂ levels in healing limb. * $p \leq 0.20$, ** $p \leq 0.005$, *** $p \leq 0.001$; $n = 6$.

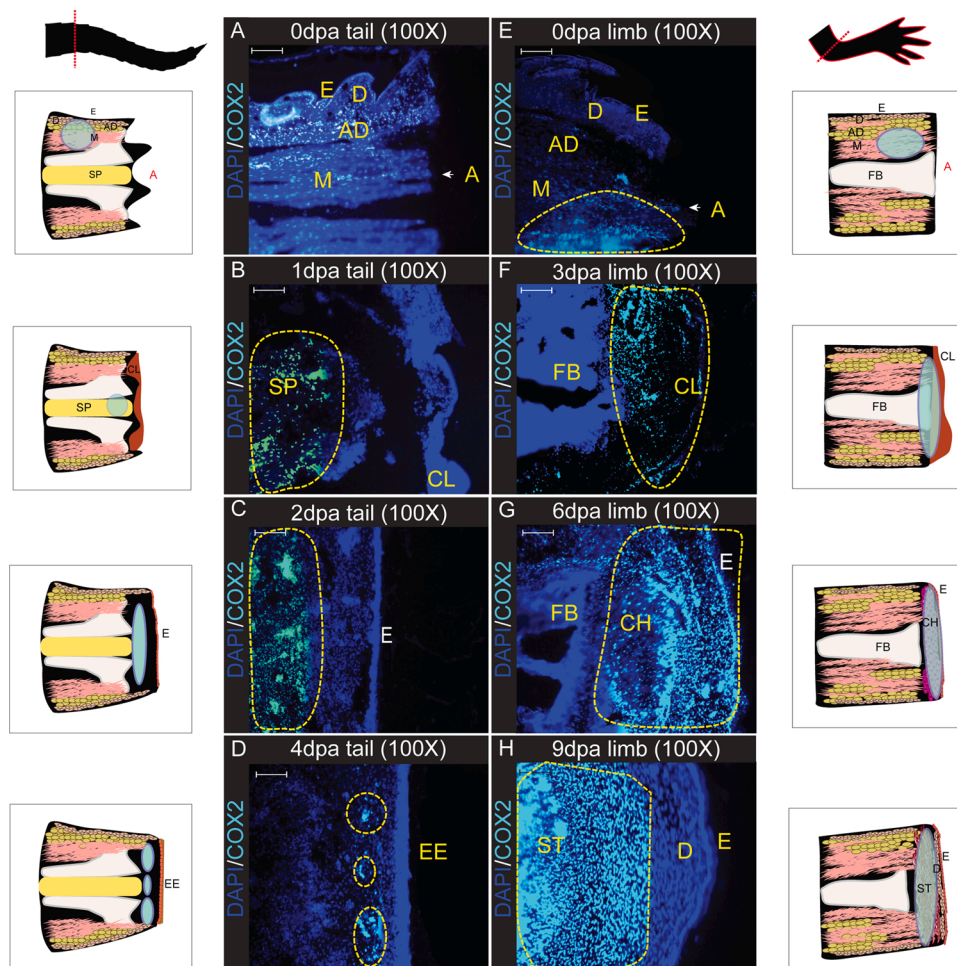


Fig. 2. Immunohistochemical localisation of COX-2: Altering intensity and sites of COX-2 localisation in the healing Tail (A-D) and Limb (E-H). Yellow dotted line depicts the site of COX-2 expression in both the tissues. A-Amputation plane; AD-Adipocyte region; EE-Epithelial Ectoderm; CH-Chondrocyte region; CL-Clot; D-Dermal region, E-Epidermal region; FB- Femur Bone; M-Muscles; SP-Spinal cord region; ST-Scar tissue; VB- Vertebral Bone. Scale bar = 200 μm . The schematic representation explains amputation plane and points out the location of COX-2 in the tissue sections, shown in cyan colour.

shown near the respective figures, to explain the exact location of COX-2, found to be temporally changing, across the healing frames of the appendages (Fig. 2). The tissue regions and cell types identified here are based on the previously reported histological details of both the appendages, in our lab (Ranadive et al., 2018).

3.4. Protein expression pattern of the inflammatory mediators in healing appendages

Protein expression was checked for the major regulators of inflammation in both tail and limb. COX-2 protein levels in the tail went up for 1 dpa, 2 dpa, 3 dpa and 4 dpa in comparison to 0 dpa (Fig. 3A; Table 2A). In limb tissue, the expression noticeably increased at 3 dpa, but maintained the same mark at 6 dpa as compared to resting stage. At 9 dpa, COX-2 protein levels remained elevated as compared to 0 dpa (Fig. 3B; Table 2B). The protein levels of EP2 receptor were found to be constantly decreasing in tail whereas in limb its levels were significantly increased from 0 dpa till 9 dpa. Alongside, protein expression of EP4 receptor was found to be increased throughout the wound healing stages of tail in comparison to resting stage (Fig. 3A; Table 2A). However, striking difference in the level of EP4 was observed in scarring limb wherein its level went down significantly from 0 dpa and continued to do so till 9 dpa (Fig. 3B; Table 2B).

Simultaneously, few pivotal proinflammatory mediators were checked for their expression, namely iNOS, TNF- α , IL-6, and IL-17. Expression levels of iNOS and TNF- α in tail were found to be reducing from 2 dpa to 4 dpa stage when compared to 0 dpa (Fig. 3A; Table 2A). On the contrary, the protein levels of iNOS and TNF- α were found to be increased during scarring in limb (Fig. 3B; Table 2B). Expression level of one of the principal anti-inflammatory mediator IL-10, was also monitored and was found to be successively increasing from 0 dpa to 4 dpa in tail (Fig. 3A; Table 2A), while its levels stooped significantly in limb after 3 dpa and remained low till 9 dpa stage (Fig. 3B; Table 2B). Protein level of IL-6 in tail was decreased starting from 1 dpa till 4 dpa in tail whereas in limb it was found to be reduced at 3 dpa however 6 dpa onwards the level increased till 9 dpa in limb. IL-17 protein levels were decreased noticeably from 1 dpa to 4 dpa in comparison to 0 dpa in tail (Fig. 3A; Table 2A). In case of limb, IL-17 protein levels were found to be decreased significantly from 0 dpa to 3 dpa, followed by a sudden rise noted for 6 dpa and 9 dpa (Fig. 3B; Table 2B). IL-22 elicited a riveting result wherein, its protein expression increased from resting stage till 4 dpa in tail. IL-22 showed marked decrease in the expression at 3 dpa

Table 2A

Band intensity (in arbitrary unit) of Western blot images of proteins probed during various healing stages of tail.

Proteins	Stages of wound healing				
	0 dpa	1 dpa	2 dpa	3 dpa	4 dpa
COX-2	123 \pm 1.60 ^a	150 \pm 0.614 ^b	151 \pm 1.35 ^b	144 \pm 2.01 ^c	143 \pm 1.30 ^c
EP2	92.9 \pm 2.36 ^a	129 \pm 1.92 ^b	140 \pm 1.72 ^c	124 \pm 2.59 ^b	118 \pm 1.45 ^c
EP4	97.5 \pm 1.18 ^a	113 \pm 1.42 ^b	127 \pm 1.38 ^c	125 \pm 2.50 ^c	130 \pm 1.15 ^c
iNOS	148 \pm 1.36 ^a	148 \pm 1.61 ^a	149 \pm 1.82 ^a	135 \pm 0.851 ^b	122 \pm 1.35 ^c
TNF- α	120 \pm 0.825 ^a	108 \pm 2.21 ^b	130 \pm 4.30 ^c	99.4 \pm 1.07 ^d	89.9 \pm 0.890 ^e
IL-10	94.1 \pm 2.31 ^a	103 \pm 1.34 ^b	106 \pm 1.30 ^b	131 \pm 3.08 ^c	122 \pm 2.32 ^d
IL-6	110 \pm 1.52 ^a	92.0 \pm 3.39 ^b	106 \pm 1.07 ^a	82.9 \pm 1.89 ^c	82.8 \pm 1.50 ^c
IL-17	151 \pm 2.92 ^a	154 \pm 1.86 ^a	144 \pm 2.42 ^b	138 \pm 3.00 ^b	123 \pm 1.38 ^c
IL-22	111 \pm 5.46 ^a	129 \pm 2.97 ^b	140 \pm 2.07 ^c	124 \pm 2.94 ^b	132 \pm 2.56 ^d
β -actin	227 \pm 2.55 ^a	225 \pm 2.98 ^a	219 \pm 3.51 ^a	219 \pm 2.90 ^a	205 \pm 9.76 ^a

Values are expressed as Mean \pm SEM; Within each row, the values sharing the same superscript are not significantly different from each other; n = 3, from a pooled sample of 6 subjects; p \leq 0.05.

Table 2B

Band intensity (in arbitrary unit) of Western blot images of proteins probed during various healing stages of limb.

Proteins	Stages of healing			
	0 dpa	3 dpa	6 dpa	9 dpa
COX-2	149 \pm 3.96 ^a	163 \pm 2.27 ^b	169 \pm 3.26 ^b	163 \pm 2.09 ^b
EP2	179 \pm 2.03 ^a	208 \pm 3.47 ^b	203 \pm 1.77 ^b	209 \pm 0.667 ^b
EP4	154 \pm 2.45 ^a	144 \pm 1.31 ^b	140 \pm 1.06 ^b	120 \pm 1.24 ^c
iNOS	108 \pm 1.65 ^a	115 \pm 1.99 ^b	106 \pm 1.41 ^a	139 \pm 4.96 ^c
TNF- α	92.3 \pm 2.04 ^a	158 \pm 1.41 ^b	136 \pm 1.89 ^c	130 \pm 1.18 ^d
IL-10	111 \pm 1.35 ^a	102 \pm 1.41 ^b	58.4 \pm 6.68 ^c	82.8 \pm 1.35 ^d
IL-6	96.6 \pm 2.37 ^a	75.5 \pm 1.67 ^b	85.6 \pm 1.48 ^c	104 \pm 2.50 ^d
IL-17	86.4 \pm 3.03 ^a	83.6 \pm 2.52 ^a	119 \pm 1.88 ^b	126 \pm 2.42 ^c
IL-22	87.1 \pm 3.75 ^a	53.7 \pm 2.06 ^b	67.4 \pm 2.57 ^c	106 \pm 4.13 ^d
β -actin	214 \pm 7.64 ^a	216 \pm 8.45 ^a	207 \pm 10.6 ^a	202 \pm 9.90 ^a

Values are expressed as Mean \pm SEM; Within each row, the values sharing the same superscript are not significantly different from each other; n = 3, from a pooled sample of 6 subjects; p \leq 0.05.

stage of healing limb but then gradually elevated at 6 dpa followed by remarkable rise at 9 dpa, when compared with 0 dpa (Fig. 3B; Table 2B).

3.5. Gene expression pattern of inflammatory mediators in healing appendages

Quantitative real-time PCR was employed to further validate the expression status of various regulatory molecules, which organise the entire inflammatory response in these two varied appendages. These molecules were majorly considered for their distinct roles, either supporting or opposing inflammation. Both tail and limb groups showed major alterations in the expression of these molecules. The genes considered were, COX-2, EP2, EP4, iNOS, TNF- α , IL-10, IL-6, IL-17 and IL-22 (Tables 3A and 3B). COX-2 is known to be upregulated under the effect of an injury, so was observed here, wherein significant elevation was observed in its transcript-level expression, under the impact of induced autotomy in the tail. Results showed a striking rise in COX-2 expression from 0 to 3 dpa by almost 16-fold which then remained 8-fold at 4 dpa in comparison to 0 dpa for the tail (Table 3A). The subjects of the limb group also showed a progressive elevation in COX-2

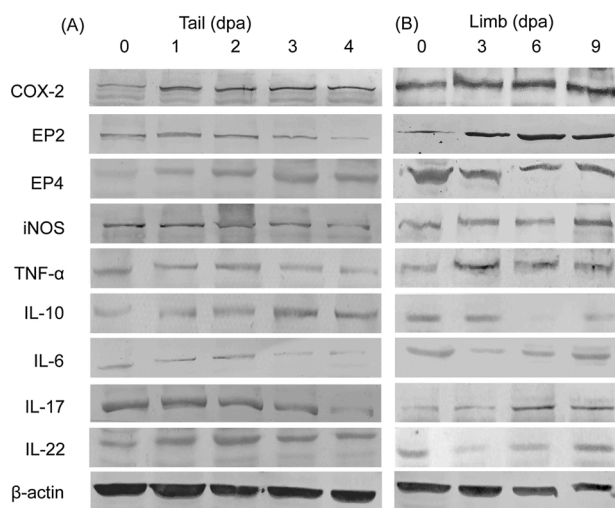


Fig. 3. Western blot panel showing the band intensity during progressive days post-amputation (dpa) for COX-2, EP2, EP4, iNOS, TNF- α , IL-10, IL-6, IL-17 and IL-22 proteins in both, healing tail and limb. β -actin was used as loading control.

Table 3A
Fold change in the expression of genes at different healing stages in tail.

Genes	Stages of healing				
	0 dpa	1 dpa	2 dpa	3 dpa	4 dpa
COX-2	1 ± 0.06 ^a	16.10 ± 0.06 ^b	16.11 ± 0.70 ^b	16.11 ± 0.68 ^b	8.35 ± 0.37 ^c
EP2	1 ± 0.05 ^a	0.40 ± 0.01 ^b	0.11 ± 0.03 ^b	0.07 ± 0.00 ^c	0.06 ± 0.00 ^d
EP4	1 ± 0.20 ^a	28.5 ± 1.28 ^b	32.9 ± 1.72 ^b	30.70 ± 1.58 ^b	25.80 ± 0.91 ^c
iNOS	1 ± 0.57 ^a	1.23 ± 0.07 ^a	0.48 ± 0.03 ^b	0.24 ± 0.03 ^c	0.10 ± 0.00 ^d
TNF-α	1 ± 0.05 ^a	1.59 ± 0.05 ^a	0.5 ± 0.03 ^b	0.69 ± 0.02 ^b	0.12 ± 0.03 ^c
IL-10	1 ± 0.00 ^a	6.89 ± 0.30 ^b	8.25 ± 0.45 ^c	12.25 ± 0.63 ^d	13.1 ± 0.58 ^d
IL-6	1 ± 0.08 ^a	0.41 ± 0.01 ^b	0.40 ± 0.01 ^b	0.23 ± 0.00 ^c	0.16 ± 0.01 ^d
IL-17	1 ± 0.07 ^a	0.22 ± 0.00 ^b	0.05 ± 0.00 ^c	0.03 ± 0.00 ^d	0.01 ± 0.00 ^e
IL-22	1 ± 0.008	2.17 ± 0.07 ^a	3.76 ± 0.18 ^b	2.03 ± 0.00 ^c	0.80 ± 0.04 ^d

Values are expressed as Mean ± SEM; Within each row, the values sharing the same superscript are not significantly different from each other; n = 3, from a pooled sample of 6 subjects; $p \leq 0.05$.

Table 3B
Fold change in the expression of genes at different healing stages in limbs.

Genes	Stages of healing			
	0 dpa	3 dpa	6 dpa	9 dpa
COX-2	1 ± 0.12 ^a	24.58 ± 1.37 ^b	31.0 ± 1.66 ^c	62.20 ± 2.89 ^d
EP2	1 ± 0.05 ^a	5.20 ± 0.02 ^b	16.11 ± 1.67 ^c	16.07 ± 0.00 ^c
EP4	1 ± 0.00 ^a	0.37 ± 0.02 ^a	0.11 ± 0.00 ^b	0.07 ± 0.00 ^b
iNOS	1 ± 0.08 ^a	3.58 ± 0.22 ^b	12.0 ± 0.66 ^c	13.12 ± 0.57 ^c
TNF-α	1 ± 0.00 ^a	2.90 ± 0.20 ^b	10.00 ± 0.66 ^c	13.30 ± 0.57 ^d
IL-10	1 ± 0.16 ^a	3.51 ± 0.15 ^b	0.12 ± 0.00 ^c	0.09 ± 0.00 ^c
IL-6	1 ± 0.11 ^a	1.23 ± 0.00 ^a	17.03 ± 0.86 ^c	25.58 ± 1.15 ^d
IL-17	1 ± 0.06 ^a	0.02 ± 0.00 ^b	12.00 ± 0.63 ^c	0.28 ± 0.00 ^d
IL-22	1 ± 0.00 ^a	0.03 ± 0.00 ^b	10.00 ± 0.05 ^c	1.05 ± 0.08 ^a

Values are expressed as Mean ± SEM; Within each row, the values sharing the same superscript are not significantly different from each other; n = 3, from a pooled sample of 6 subjects; $p \leq 0.05$.

mRNA from 0 to 9 dpa (Table 3B).

Additionally, the level of EP2, a member of the PGE₂ receptor family, was checked, which showed noticeable variation in expression. The EP2 gene expression was in concurrence with its protein expression data wherein the levels were decreased throughout the course of healing in tail (Table 3A) and were upregulated in scarring limb (Table 3B). Another PGE₂ receptor, EP4 was checked and it elicited rise in gene expression at 1 dpa and remained elevated till 4 dpa, when compared to 0 dpa (Table 3A). On the limb front though, it decreased significantly at 3 dpa which remained persistent till 9 dpa as well (Table 3B).

Various proinflammatory mediators, boosting the course of inflammation were checked, namely- iNOS, TNF-α and IL-6, for their temporal gene expression pattern. All these three genes showed prominent reduction from 1 dpa till 4 dpa as compared to 0 dpa during lizard tail regeneration (Table 3A). However, during limb healing, iNOS, TNF-α and IL-6 transcript levels were upregulated remarkably in comparison to 0 dpa (Table 3B). Thus, iNOS, TNF-α, and IL-6, all showed progressive reduction in expression during the course of wound healing in tail, while the anti-inflammatory mediators IL-10 showed increase of expression (Table 3A). Herein, conspicuous rise in its gene expression was recorded from 1 dpa onwards, which progressed across 2, 3 and 4 dpa stages to increase by 13-folds at the terminal time point, as compared to the resting one (Table 3A). On the contrary, a significant reduction in its expression was observed at the 6 dpa of limb, after a marked elevation at

3 dpa, followed by remarkable decrease at the final time point of 9 dpa (Table 3B). Thus, subjects of the limb group, showed exact contrast, to the tail group, with respect to the trend of gene expression, as the proinflammatory mediators displayed a prominent rise while the anti-inflammatory molecule elicited evident reduction (Tables 3A and 3B).

Apart from these genes, we found specific changes in the status of IL-17 and IL-22 gene expressions. During our study we found IL-17, to be reducing in an ordered fashion, in the tail tissues (Table 3A). Initially, it promiscuously rose from 0 to 2 dpa and suddenly stooped down by 3 dpa, also staying down by the end of 4 dpa. In such an environment, IL-22 portrayed a constructive character and supported the fast-healing process of the tail, possibly because its levels also increased till 2 dpa as compared to the resting stage, followed by peculiar heightened numbers at 3 dpa, which only reduced significantly at the last time point studied, i.e., 4 dpa (Table 3A).

On the other hand, in the case of the limb, IL-17 showed a major reduction in gene expression at 3 dpa followed by a significant hike at 6 dpa, which reduced again at 9 dpa, as compared to 0 dpa. Congruently, IL-22 transcripts too reduced remarkably at 3 dpa followed by a sudden hike at 6 dpa, while it returned to near basal level at 9 dpa, when compared to the resting stage (Table 3B).

4. Discussion

This study is a diligent attempt to highlight the involvement and impact of inflammation on wound healing of lizard appendages, viz., tail and limb. As per our prevalent knowledge of over many decades now, cyclooxygenase, is a family of enzymes, which regulates and fine-tunes multiple developmental programmes like cell survival, proliferation and migration (Lu et al., 1995; Dubois et al., 1998; Simmons et al., 2004; Liou et al., 2007). The results obtained here suggest that COX-2, an inducible isoform of COX, plausibly modulates inflammation through varied PGE₂-EP receptor signalling, wherein specific interleukins are recruited at the site of repair.

COX-2 activity elevated 2 dpa onwards in lizard tail, while in limb it was relatively high and increased progressively at the following time points. As COX-2 belongs to the family of early response genes and is strongly induced by mitogenic and proinflammatory stimuli (Lasa et al., 2000), in the next step, protein and transcript levels of COX-2 were checked. In resemblance to its hiked activity, COX-2 protein and gene levels were also found to be elevated till the 3 dpa stage in tail. This suggests participation of COX-2 in modulating early inflammation, which reduced at 4 dpa, during proliferation and epithelialisation. On the contrary, in limbs COX-2 gene expression increased from the basal level till the terminal time point of 9 dpa. This suggests mRNA stabilisation in limb tissue, due to elevated proinflammatory interleukins as found in human bones, macrophages and granulosa cells by Kang et al. (Kang et al., 2007)

Further COX-2 activity forms PGE₂ as an early response gene product, boosted by proinflammatory cytokines, governing its transcriptional and post-transcriptional levels (Kang et al., 2007). PGE₂ expression followed a trend of COX-2 activity in tail, while in limb, it showed significant decrease after 3 dpa, until 9 dpa. Interestingly, the basal level of PGE₂ in limb (0 dpa) is higher than the terminal time point for tail (9 dpa). This disparity could be a function of COX-2 driving multiple signalling pathways in various tissues in a context specific manner (DuBois et al., 1998; Simmons et al., 2004; Tsatsanis et al., 2006). Also, other tissue specific inflammation curbing prostanoids might participate to cause early resolution and resultant super healing in tail, while contrasting results are observed in limb (Bos et al., 2004; Korbecki et al., 2014). Meanwhile, a complete profiling of all prostanoids participating in these events, would explain their roles in regulation of inflammation.

Aoki and Narumiya (2017), have established that PGE₂ and its interaction with the downstream receptor (EP1-4) (Minami et al., 2001), determines the course of inflammation in the healing tissue. Also, the

intracellular messengers such as, cAMP and phospho- CREB function under the EP2 and EP4 activation to cause a hike in gene and protein levels of proinflammatory cytokines, which then support inflammation by regulating both, its manifestation and resolution (Smith, 1992; Bos et al., 2004; Sugimoto and Narumiya, 2007).

Present results suggest a similar tissue specific PGE₂-EP receptor action, as in tail, along with EP2, IL-6, a major proinflammatory mediator got alleviated. On the other hand, in limb, EP2 levels elevated for both protein and gene expression, along with steady rise in the levels of the major proinflammatory mediators such as iNOS, TNF- α and IL-6. The correlation of the EP2 receptors with the downstream proinflammatory mediators has been reported earlier too (Hinson et al., 1996; Aoki and Narumiya, 2017). On the contrary, the antiinflammatory action of EP4 has also been reported in a wide array of systems (Heffron et al., 2020; Joshi et al., 2020; Yasui-Kato et al., 2020). In the present model too, this evident contrast in the EP2-EP4 expression pattern could be the primary reason for the exquisite dissimilarity in the status of inflammation. This contrasting appearance and action of the two receptors, might recruit differential cluster of either anti or proinflammatory mediators at the site of wound healing in tail and limb, respectively.

Major proinflammatory mediators, iNOS, TNF- α , IL-6, etc work in congruence to promote the tissue-specific inflammation at the site of injury, while they function as per the COX-2 mediated PGE₂ expression and its binding with the downstream EP receptors (Hinson et al., 1996; Harris et al., 2002). It is the stark difference in the levels of these regulators (PGE₂ and EP receptors) and their periodic expression, which possibly lays the foundation of biased wound healing in the two appendages.

TNF- α is a well-established proinflammatory mediator (Lawrence, 2009), that functions in coherence with PGE₂ and recruits other inflammation boosting interleukins such as IL-6 (Hinson et al., 1996) and rising expression of this prostaglandin as well (Harris et al., 2002). In the present study, TNF- α and IL-6 show distinct decline in the gene and protein expression in tail, overlapping haemostasis and epithelialisation stages of wound healing. These levels further stoop during the proliferative phase by the fourth day of amputation. On the contrary, in limbs, TNF- α and IL-6 showed continuous rise till 9 dpa, confirming the prolonged high levels of inflammation in the microenvironment. Along with these proinflammatory cytokines, their antiinflammatory counterparts are also recruited, which form the necessary balance for the successful tissue repair (Renz et al., 1988; Hinson et al., 1996; Ricciotti and Fitzgerald, 2011). In present results, gene and protein levels of a major antiinflammatory mediator IL-10 spiked significantly in the tail but reduced during the healing course in limb. This substantial disparity in expression could be responsible for early and delayed epithelialisation found in tail (Fig. 2B-C) and limb (Fig. 2F-H), respectively. Peranteau et al. (2008) have reported the positive effect of IL-10 overexpression in an adult mice model of regeneration. The collaborative functions of the EP2 and EP4 receptors, which recruit and regulate these cytokines during wound healing (Hinson et al., 1996; Portanova et al., 1996; Harris et al., 2002; Harizi et al., 2003), could be responsible for its differential outcome.

However, with respect to the transcript and protein, the most striking observations were made for IL-17 and IL-22. Through studies of IL-17 KO mice, Yang et al. (2008) have proven its major role in inducing inflammation that positively leads to tissue remodelling. Remarkably, this is for the first time that its role is being revealed in a the animal model of appendage regeneration. Its differential behaviour is studied here in two contrasting tissues, which have taken opposite paths of wound healing. IL-17 showed significant reduction in gene expression traversing all the time points, for tail group, after the early inflammation (2 dpa). This supports the idea that reduction of chief proinflammatory mediators cause an overall decline of inflammation at tissue level in tail and promote regeneration supportive wound healing (Fig. 2A-D). As opined by Veldhoen et al. (2006), reduction in IL-17 expression in tail is a coherent effect of another regulatory mediator like IL-6 which has

shown a major decline here. It could even be due to the specific signalling dictated by the EP receptors (Hinson et al., 1996). In limb tissue though, IL-17 was elevated, except at the time when scar formation and collagen deposition start at the site of healing (Fig. 2H). This disparity could be simply because by the end of scab formation, a permanent scar is constructed via collagen deposition and recruitment of fibroblast cells (Ranadive et al., 2018), while the tissue inflammation recedes to enhance the former process. Discovering this novel participation of IL-17 in the regeneration model recommends further investigation, where the performance of this cardinal inflammatory mediator can be explored.

IL-22, in the tail tissue showed well pronounced increase in its transcripts from 1 dpa till 3 dpa, after which its level reduced significantly by 4 dpa. This ensures its participation in early epithelialisation, as achieved in tail. IL-22 elicits a protective role, when combined with IL-17, which specifically induces anti-microbial peptides in human keratinocytes (Sabat et al., 2013). Moreover, reduction of IL-17 could possibly influence the levels of IL-22 as observed in few other models like human T-cells (Veldhoen et al., 2006). This could be majorly because it is a cytokine of IL-10 superfamily, levels of which plunge under excessive inflammation (Zheng et al., 2007), as observed here in case of limb tissues. Herein, IL-22 followed the trend of IL-17, with noticeable rise in gene expression at the time of scab formation in limb tissue, in congruence with other proinflammatory mediators like IL-6, TNF- α , iNOS and IL-17. It is thus proved that IL-22 plays its part in repairing the wound in the two appendages, in synergy with IL-17 and reconstructs the framework for scar-free healing in tail (Fig. 2D), however, it supports scar formation (Fig. 2H) under the prolonged inflammatory response in limb.

Overall, this is an inquisitive effort to deduce the crosstalk between inflammation and the colossal course of events leading to differential wound healing in lizard. These findings reinforce the concept that inflammation can hinder the restoration proceedings if its elevated levels remain persistent for a longer duration of time (Mescher et al., 2013). The COX-2 mediated PGE₂ might play a pivotal role in symphonising the entire event of the inflammation as it operates and directs the interleukin function at the site of tissue repair. COX-2-PGE₂-EP receptor cascade plausibly governs both, restoration of lost tissue via scar-free wound healing or a permanent scar formation at the locale of injury. Hence, this study again establishes the dual role of inflammation in boosting and banishing the regenerative process.

5. Conclusion

COX-2 derived PGE₂ might alter the expression of inflammatory mediators depending upon the receptor action downstream. The mediators of inflammation, both supporting and inhibiting its progression, are recruited at the site of healing in an appendage specific fashion. Reduction in inflammation due to PGE₂-EP4 dependant rise in IL-10 causes scar-free repair in the tail, supporting regenerative outcome. However, in limb, elevated levels of proinflammatory mediators based on PGE₂-EP2 action support scar formation instead. Illustrating the contribution of these mediators here would help us further explore the course of action deployed by these molecules in future studies.

Ethics approval and consent to participate

The experimental protocol (MSU-Z/IAEC/15-2017) was approved by the Institutional Animal Ethics Committee (IAEC) and all the experiments were performed as per the guidelines of Committee for the Purpose of Control and Supervision of Experiments on Animals (CPCSEA), India.

Consent for publication

Not applicable

Availability of data and material

Not applicable

Funding

The work was supported by grants from Department of Biotechnology, Ministry of Science and Technology, India (BT/PR11467/MED/31/270/2014; Dt- 02/09/2016).

Authors' contributions

BS conceived and strategized the study. KK, PB and UV were responsible for acquisition of the data. KK, UV and SP analysed the data. The manuscript has been drafted by KK and UV and critically reviewed by IR, PB and BS. All authors have read and approved the final manuscript.

Declaration of Competing Interest

The authors report no declarations of interest.

Acknowledgement

KK is deeply obliged to DBT for providing fellowship.

References

- Agata, K., Saito, Y., Nakajima, E., 2007. Unifying principles of regeneration I: Epimorphosis versus morphallaxis. *Dev. Growth Differ.* 49, 73–78. <https://doi.org/10.1111/j.1440-169X.2007.00919.x>.
- Alibardi, L., 2014. Histochemical, Biochemical and Cell Biological aspects of tail regeneration in lizard, an amniote model for studies on tissue regeneration. *Progress Histochem. Cytochem.* 48 (4), 143–244.
- Aoki, T., Narumiya, S., 2017. Prostaglandin E 2-EP2 signaling as a node of chronic inflammation in the colon tumor microenvironment. *Inflamm. Regen.* 37, 4. <https://doi.org/10.1186/s41232-017-0036-7>.
- Bely, A., 2010. Evolutionary loss of animal regeneration: pattern and process. *Integr. Comp. Biol.* 50, 515–527. <https://doi.org/10.1093/icb/118>.
- Bos, C., Richel, D., Ritsema, T., Peppelenbosch, M., Versteeg, H., 2004. Prostanoids and prostanoid receptors in signal transduction. *Int. J. Biochem. Cell Biol.* 36, 1187–1205. <https://doi.org/10.1016/j.biocel.2003.08.006>.
- Bradford, M., 1976. A rapid and sensitive method for the quantitation of microgram quantities of protein utilizing the principle of protein-dye binding. *Anal. Biochem.* 72, 248–254. [https://doi.org/10.1016/0003-2697\(76\)90527-3](https://doi.org/10.1016/0003-2697(76)90527-3).
- Buch, P., Desai, I., Balakrishnan, S., 2018. COX-2 activity and expression pattern during regenerative wound healing of tail in lizard *Hemidactylus flaviviridis*. *Prostaglandin and Other Lipid Mediators* 135, 11–15. <https://doi.org/10.1016/j.prostaglandins.2018.01.002>.
- Buch, P., Sarkate, P., Uggini, G., Desai, I., Balakrishnan, S., 2017. Inhibition of cyclooxygenase-2 alters Wnt/ β -catenin signaling in the regenerating tail of lizard *Hemidactylus flaviviridis*. *Tissue Eng. Regen. Med.* 14, 171–178. <https://doi.org/10.1007/s13770-017-0037-2>.
- Chamberlain, C., Leiferman, E., Frisch, K., Brickson, S., Murphy, W., Baer, G., Vanderby, R., 2013. Interleukin expression after injury and the effects of interleukin-1 receptor antagonist. *PLoS One* 8, e71631. <https://doi.org/10.1371/journal.pone.0071631>.
- Dubois, R., Abramson, S., Crofford, L., Gupta, R., Simon, L., Van De Putte, L., Lipsky, P., 1998. Cyclooxygenase in biology and disease. *The FASEB J.* 12, 1063–1073. <https://doi.org/10.1096/fasebj.12.12.1063>.
- Gilbert, E., Delorme, S., Vickaryous, M., 2015. The regeneration blastema of lizards: an amniote model for the study of appendage replacement. *Regen.* 2, 45–53. <https://doi.org/10.1002/reg.2.31>.
- Harizi, H., Grosset, C., Gualde, N., 2003. Prostaglandin E2 modulates dendritic cell function via EP2 and EP4 receptor subtypes. *J. Leukoc. Biol.* 73, 756–763. <https://doi.org/10.1189/jlb.1002483>.
- Harris, S., Padilla, J., Koumas, L., Ray, D., Phipps, R., 2002. Prostaglandins as modulators of immunity. *Trends Immunol.* 23, 144–150. [https://doi.org/10.1016/S1471-4906\(01\)02154-8](https://doi.org/10.1016/S1471-4906(01)02154-8).
- Heffron, S., Weinstock, A., Scolaro, B., Chen, S., Sansbury, B., Marecki, G., Rolling, C., El Bannoudi, H., Barrett, T., Canary, J.W., Spite, M., Berger, J., Fisher, A., 2020. Platelet-conditioned media induces an anti-inflammatory macrophage phenotype through EP4. *J. Thromb. Haemost.* 19, 562–573. <https://doi.org/10.1111/jth.15172>.
- Hinson, R., Williams, J., Shacter, E., 1996. Elevated interleukin 6 is induced by prostaglandin E2 in a murine model of inflammation: possible role of cyclooxygenase-2. *Proc. Natl. Acad. Sci.* 93, 4885–4890. <https://doi.org/10.1073/pnas.93.10.4885>.
- Joshi, R., Hamed, O., Yan, D., Michi, A., Mostafa, M., Wiehler, S., Newton, R., Giembycz, M., 2020. Prostanoid receptors of the EP4-subtype mediate gene expression changes in human airway epithelial cells with potential anti-inflammatory activity. *J. Pharm. Exp. Ther.* 376, 161–180. <https://doi.org/10.1124/jpet.120.000196>.
- Kaiser, P., Rothwell, L., Avery, S., Balu, S., 2004. Evolution of the interleukins. *Dev. Comp. Immunol.* 28, 375–394. <https://doi.org/10.1016/j.dci.2003.09.004>.
- Kang, Y., Mbonye, U., DeLong, C., Wada, M., Smith, W., 2007. Regulation of intracellular cyclooxygenase levels by gene transcription and protein degradation. *Progress in Lipid Research.* 46, 108–125. <https://doi.org/10.1016/j.plipres.2007.01.001>.
- Karin, M., Clevers, H., 2016. Reparative inflammation takes charge of tissue regeneration. *Nature.* 529, 307–315. <https://doi.org/10.1038/nature17039>.
- Korbecki, J., Baranowska-Bosiacka, I., Gutowska, I., Chlubek, D., 2014. Cyclooxygenase pathways. *Acta Biochim. Pol.* 61 (4) <https://doi.org/10.18388/abp.2014.1825>.
- Lasa, M., Mahtani, K., Finch, A., Brewer, G., Saklatvala, J., Clark, A., 2000. Regulation of cyclooxygenase 2 mRNA stability by the mitogen-activated protein kinase p38 signaling cascade. *Mol. Cell. Biol.* 20, 4265–4274. <https://doi.org/10.1128/MCB.20.12.4265-4274.2000>.
- Lawrence, T., 2009. The nuclear factor NF- κ B pathway in inflammation. *Cold Spring Harbor perspectives in Biology.* 1, a001651 <https://doi.org/10.1101/cshperspect.a001651>.
- Liou, J., Ellent, D., Lee, S., Goldsby, J., Ko, B., Matijevic, N., Huang, J.C., Wu, K., 2007. Cyclooxygenase-2-derived prostaglandin e2 protects mouse embryonic stem cells from apoptosis. *Stem Cells.* 25 (5), 1096–1103. <https://doi.org/10.1634/stemcells.2006-0505>.
- Livak, K., Schmittgen, T., 2001. Analysis of relative gene expression data using real-time quantitative PCR and the 2⁻ $\Delta\Delta$ CT method. *Methods.* 25, 402–408. <https://doi.org/10.1006/meth.2001.1262>.
- Lu, X., Xie, W., Reed, D., Bradshaw, W., Simmons, D., 1995. Nonsteroidal antiinflammatory drugs cause apoptosis and induce cyclooxygenases in chicken embryo fibroblasts. *Proc. Natl. Acad. Sci.* 92, 7961–7965. <https://doi.org/10.1073/pnas.92.17.7961>.
- Mescher, A., Neff, A., King, M., 2013. Changes in the inflammatory response to injury and its resolution during the loss of regenerative capacity in developing *Xenopus* limbs. *PLoS One.* 8, e80477 <https://doi.org/10.1371/journal.pone.0080477>.
- Minami, T., Nakano, H., Kobayashi, T., Sugimoto, Y., Ushikubi, F., Ichikawa, A., Narumiya, S., Ito, S., 2001. Characterization of EP receptor subtypes responsible for prostaglandin E2-induced pain responses by use of EP1 and EP3 receptor knockout mice. *Brit. J. Pharma.* 133, 438–444. <https://doi.org/10.1038/sj.bjp.0704092>.
- Murphy, B., Thompson, M., 2011. A review of the evolution of viviparity in squamate reptiles: the past, present and future role of molecular biology and genomics. *J. Comp. Physiol. B.* 181, 575–594. <https://doi.org/10.1007/s00360-011-0584-0>.
- Parmar, B., Verma, U., Khaire, K., Danes, D., Balakrishnan, S., 2021. Inhibition of cyclooxygenase-2 alters craniofacial patterning during early embryonic development of chick. *J. Dev. Biol.* 9, 16.
- Peranteau, W., Zhang, L., Muvarak, N., Badillo, A., Radu, A., Zoltick, P.W., Liechty, K., 2008. IL-10 overexpression decreases inflammatory mediators and promotes regenerative healing in an adult model of scar formation. *J. Investig. Dermatol.* 128, 1852–1860. <https://doi.org/10.1038/sj.jid.5701232>.
- Portanova, J., Zhang, Y., Anderson, G., Hauser, S., Masferrer, J., Seibert, K., Gregory, S., Isakson, P., 1996. Selective neutralization of prostaglandin E2 blocks inflammation, hyperalgesia, and interleukin 6 production in vivo. *J. Exp. Med.* 184, 883–891. <https://doi.org/10.1084/jem.184.3.883>.
- Prisk, V., Huard, J., 2003. Muscle injuries and repair: the role of prostaglandins and inflammation. *Histol. and Histopathol.* 18, 1243–1256. <https://doi.org/10.14670/HH-18.1243>.
- Ranadive, I., Patel, S., Buch, P., Uggini, G., Desai, I., Balakrishnan, S., 2018. Inherent variations in the cellular events at the site of amputation orchestrate scar-free wound healing in the tail and scarred wound healing in the limb of lizard *Hemidactylus flaviviridis*. *Wound Rep. Regen.* 26, 366–380. <https://doi.org/10.1111/wrr.12659>.
- Renz, H., Gong, J., Schmidt, A., Nain, M., Gamsa, D., 1988. Release of tumor necrosis factor- α from macrophages. Enhancement and suppression are dose-dependently regulated by prostaglandin E2 and cyclic nucleotides. *J. Immunol.* 141, 2388–2393.
- Ricciotti, E., FitzGerald, G., 2011. Prostaglandins and inflammation. *Arterio. Thromb. Vasc. Biol.* 31, 986–1000. <https://doi.org/10.1161/ATVBAHA.110.207449>.
- Sabat, R., Witte, E., Witte, K., Wolk, K., 2013. IL-22 and IL-17: an overview. IL-17, IL-22 and their producing cells: Role in Inflammation and Autoimmunity. Springer, Basel, pp. 11–35.
- Sharma, P., Suresh, B., 2008. Influence of COX-2-Induced PGE. *Folia Biol. (Praha)* 54, 193–201.
- Simmons, D., Botting, R., Hla, T., 2004. Cyclooxygenase isozymes: the biology of prostaglandin synthesis and inhibition. *Pharma. Rev.* 56, 387–437. <https://doi.org/10.1124/pr.56.3.3>.
- Smith, R., 1992. A comprehensive macrophage-T-lymphocyte theory of schizophrenia. *Med. Hypotheses.* 39, 248–257. [https://doi.org/10.1016/0306-9877\(92\)90117-U](https://doi.org/10.1016/0306-9877(92)90117-U).
- Sugimoto, Y., Narumiya, S., 2007. Prostaglandin E receptors. *J. Biol. Chem.* 282, 11613–11617. <https://doi.org/10.1074/jbc.R600038200>.
- Suzuki, M., Yakushiji, N., Nakada, Y., Satoh, A., Ide, H., Tamura, K., 2006. Limb regeneration in *Xenopus laevis* froglet. *Sci. World J.* 6 <https://doi.org/10.1100/tsw.2006.325>.
- Tsatsanis, C., Androulidaki, A., Venihaki, M., Margioris, A., 2006. Signalling networks regulating cyclooxygenase-2. *Int. J. Biochem. Cell Biol.* 38, 1654–1661. <https://doi.org/10.1016/j.biocel.2006.03.021>.

- Veldhoen, M., Hocking, R., Atkins, C., Locksley, R., Stockinger, B., 2006. TGF β in the context of an inflammatory cytokine milieu supports de novo differentiation of IL-17-producing T cells. *Immunity*. 24, 179–189. <https://doi.org/10.1016/j.immuni.2006.01.001>.
- Verma, U., Gautam, M., Parmar, B., Khaire, K., Wishart, D., Balakrishnan, S., 2021. New insights into the obligatory nature of cyclooxygenase-2 and PGE2 during early chick embryogenesis. *BBA- Mol. Cell Biol. Lipids* 1886. <https://doi.org/10.1016/j.bbalip.2021.158889>.
- Vervoort, M., 2011. Regeneration and development in animals. *Biol. Theory*. 6, 25–35. <https://doi.org/10.1007/s13752-011-0005-3>.
- Vitolo, N., Dalla Valle, L., Skobo, T., Valle, G., Alibardi, L., 2017. Transcriptome analysis of the regenerating tail vs. the scarring limb in lizard reveals pathways leading to successful vs. unsuccessful organ regeneration in amniotes. *Dev. Dyn.* 246, 116–134. <https://doi.org/10.1002/dvdy.24474>.
- Yang, X., Chang, S., Park, H., Nurieva, R., Shah, B., Acero, L., Wang, Y., Kimberly, S., Broaddus, R., Zhu, Z., Dong, C., 2008. Regulation of inflammatory responses by IL-17F. *J. Exp. Med.* 205, 1063–1075. <https://doi.org/10.1084/jem.20071978>.
- Yasui-Kato, M., Patlada, S., Yokode, M., Kamei, K., Minami, M., 2020. EP4 signalling is essential for controlling islet inflammation by causing a shift in macrophage polarization in obesity/type 2 diabetes. *Diabetes and Vasc. Dis. Res.* 17 <https://doi.org/10.1177/1479164120945675>, 1479164120945675.
- Zheng, Y., Danilenko, D., Valdez, P., Kasman, I., Eastham-Anderson, J., Wu, J., Ouyang, W., 2007. Interleukin-22, a TH 17 cytokine, mediates IL-23-induced dermal inflammation and acanthosis. *Nature* 445, 648–651. <https://doi.org/10.1038/nature05505>.

Article

Inhibition of Cyclooxygenase-2 Alters Craniofacial Patterning during Early Embryonic Development of Chick

Bhaval Parmar, Urja Verma, **Kashmira Khaire**, Dhanush Danes and Suresh Balakrishnan * 

Department of Zoology, Faculty of Science, The Maharaja Sayajirao University of Baroda, Gujarat 390002, India; bhaval.p-zoophd@msubaroda.ac.in (B.P.); urja.verma-zoophd@msubaroda.ac.in (U.V.); kashmira.k-zoophd@msubaroda.ac.in (K.K.); dhanush.danes-zoo@msubaroda.ac.in (D.D.)

* Correspondence: b.suresh-zoo@msubaroda.ac.in

Abstract: A recent study from our lab revealed that the inhibition of cyclooxygenase-2 (COX-2) exclusively reduces the level of PGE₂ (Prostaglandin E₂) among prostanoids and hampers the normal development of several structures, strikingly the cranial vault, in chick embryos. In order to unearth the mechanism behind the deviant development of cranial features, the expression pattern of various factors that are known to influence cranial neural crest cell (CNCC) migration was checked in chick embryos after inhibiting COX-2 activity using etoricoxib. The compromised level of cell adhesion molecules and their upstream regulators, namely CDH1 (E-cadherin), CDH2 (N-cadherin), MSX1 (Msh homeobox 1), and TGF- β (Transforming growth factor beta), observed in the etoricoxib-treated embryos indicate that COX-2, through its downstream effector PGE₂, regulates the expression of these factors perhaps to aid the migration of CNCCs. The histological features and levels of FoxD3 (Forkhead box D3), as well as PCNA (Proliferating cell nuclear antigen), further consolidate the role of COX-2 in the migration and survival of CNCCs in developing embryos. The results of the current study indicate that COX-2 plays a pivotal role in orchestrating craniofacial structures perhaps by modulating CNCC proliferation and migration during the embryonic development of chicks.

Keywords: cranial neural crest cells; embryogenesis; development; cell migration



Citation: Parmar, B.; Verma, U.; Khaire, K.; Danes, D.; Balakrishnan, S. Inhibition of Cyclooxygenase-2 Alters Craniofacial Patterning during Early Embryonic Development of Chick. *J. Dev. Biol.* **2021**, *9*, 16. <https://doi.org/10.3390/jdb9020016>

Academic Editors: Simon J. Conway and Sally Moody

Received: 27 February 2021

Accepted: 20 April 2021

Published: 23 April 2021

Publisher's Note: MDPI stays neutral with regard to jurisdictional claims in published maps and institutional affiliations.

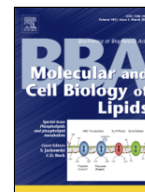


Copyright: © 2021 by the authors. Licensee MDPI, Basel, Switzerland. This article is an open access article distributed under the terms and conditions of the Creative Commons Attribution (CC BY) license (<https://creativecommons.org/licenses/by/4.0/>).

1. Introduction

Craniofacial development involves the formation of cranial neural crest cells (CNCCs) via epithelial–mesenchymal transition (EMT), induction, delamination, and migration, followed by the morphogenesis of various organs of an organism [1]. The above-mentioned events are tightly regulated by several genes that coordinate for craniofacial formation and patterning [2]. CNCCs are clusters of multipotent cells and fate-restricted progenitors that can differentiate into a multitude of tissue types based on the molecular signals they receive [3]. Their precursors undergo EMT and migrate from the forebrain, midbrain, and rhombomeres of the hindbrain to populate at the pharyngeal arches and contribute to the patterning of head and face structures. Once CNCCs pass through the EMT process, they begin migration. During migration, they proliferate and increase the pool of cells. The whole process of CNCC migration and proliferation is governed by various signaling pathways such as Fgf (Fibroblast growth factors), Wnt (Wingless-related integration site), TGF- β , and BMP (Bone morphogenetic protein) [3,4]. When the migration or differentiation of CNCCs is disrupted, defects of descendant tissues occur, which result in craniofacial malformations, the most common birth defect in humans [5].

Based on studies involving a wide array of model organisms, it can be construed that the molecular organizers of CNCC migration are conserved across various classes of vertebrates [4,6,7]. The canonical Wnt/ β -catenin signaling pathway is reported to play a major role in the formation and progression of CNCCs, as it influences both delamination and migration by interacting with BMP4 and TGF- β , respectively [8–11]. Delamination is a collective effort orchestrated by downstream targets of Wnt3A and BMP4 signaling.



New insights into the obligatory nature of cyclooxygenase-2 and PGE₂ during early chick embryogenesis

Urja Verma^a, Maheswor Gautam^b, Bhaval Parmar^a, Kashmira Khaire^a, David S. Wishart^{b,c}, Suresh Balakrishnan^{a,*}

^a Department of Zoology, Faculty of Science, The Maharaja Sayajirao University of Baroda, Gujarat 390 002, India

^b Department of Biological Sciences, University of Alberta, Edmonton, AB T6G 2E9, Canada

^c Department of Computing Science, University of Alberta, Edmonton, AB T6G 2E9, Canada

ARTICLE INFO

Keywords

Cyclooxygenase
Embryogenesis
Prostaglandins
Lipids
Development

ABSTRACT

Temporal expression patterns and activity of two cyclooxygenase (COX-1 and COX-2) isoforms were analysed during early chick embryogenesis to evaluate their roles in development. COX-2 inhibition with etoricoxib resulted in significant structural anomalies such as anophthalmia (born without one or both eyes), phocomelia (underdeveloped or truncated limbs), and gastroschisis (an opening in the abdominal wall), indicating its significance in embryogenesis. Furthermore, the levels of PGE₂, PGD₂, PGF_{2α}, and TXB₂ were assessed using quantitative LC-MS/MS to identify which effector prostanoid (s) had their synthesis initiated by COX-2. COX-2 inhibition was only shown to reduce the level of PGE₂ significantly, and hence it could be inferred that the later could be largely under the regulation of activated COX-2 in chick embryos. The compensatory increase in the activity of COX-1 observed in the etoricoxib-treated group helped to maintain the levels of PGD₂, PGF_{2α}, and TXB₂. Though the roles of these three prostanoids in embryogenesis need to be further clarified, it appears that their contribution to the observed developmental anomalies is minimal. This study has shown that COX-2 is functionally active during chick embryogenesis, and it plays a central role in the structural configuration of several organs and tissues through its downstream effector molecule PGE₂.

1. Introduction

Cyclooxygenase enzymes, which exist in two isoforms (COX-1 and COX-2), convert arachidonic acid from the plasma membrane into various prostanoids such as prostaglandins (PGs) and thromboxanes (TXs) [1]. Typically, of these two isoforms, COX-2 is considered to be the inducible type, whereas COX-1 is considered as the constitutive one. Both these isoforms are stimulated during inflammation to initiate the production of prostanoids, whereupon specific prostanoids are produced with the help of tissue-specific prostaglandin synthases to perform particular functions regionally [1]. The roles of COX-2 and the derived prostanoids have been elucidated through the genetic modification and pharmacological inhibition of the enzyme [2,3]. The majority of investigations over the past decade have focused on the role of COX-2 in tumorigenesis, which has certainly helped in understanding the aetiology of several cancers [3,4]. On the contrary, only a handful of studies have explored the involvement of prostaglandins induced via COX-2 in embryogenesis and other developmental processes. Essentiality of COX-2 in facilitating appendage regeneration via modulation of the expression of WNT, FGF, and MMP has been recently identified in reptiles [5,6]. COX-2 induced PGs are also known to be actively functioning for

ovulation, fertilisation, decidualisation, and implantation in mammals [7,8]. More recently, COX-2 was found to interfere with blastocyst hatching, a prelude to successful implantation, in hamsters [9]. Additionally, Loftin and colleagues reported COX-2 to be necessary for the closure of ductus arteriosus in mice [2]. Likewise, the ubiquitous expression of COX-2 in early stages of embryonic development has been shown to result in skeletal deformities in a novel COX-2 transgenic mouse model [10]. In an effort to understand what tissues might be affected, Stanfield and colleagues (2002) localised COX-2 in rat embryonic, and foetal tissues, wherein its presence was found in the heart, kidney, skin, and cartilage [11]. These studies indeed suggest that COX-2, either through its inhibition or activation, could have an effect on the development of a number of organs, organ systems or tissues in vertebrates.

In the present study, we ascertained the expression of COX-2 in the chick embryos during the first ten days of development by measuring its mRNA levels, protein levels, and enzymatic activity. Chick embryos do not show inflammation until after three weeks of development [12], and thus this model is ideal for studying the non-inflammatory roles of COX-2. After ascertaining its normal basal level, the activity of COX-2 was inhibited to understand its plausible roles in organ and limb forma-

* Corresponding author.

E-mail address: b.suresh-zoo@msubaroda.ac.in (S. Balakrishnan)

Early embryonic exposure to chlorpyrifos-cypermethrin combination induces pattern deficits in the heart of domestic hen

Urja Verma | **Kashmira Khaire** | Isha Desai | Shashikant Sharma |
Suresh Balakrishnan

Department of Zoology, Faculty of Science,
The Maharaja Sayajirao University of Baroda,
Vadodra, India

Correspondence

Suresh Balakrishnan, Department of Zoology,
Faculty of Science, The Maharaja Sayajirao
University of Baroda, Vadodra 390 002.
Email: b.suresh-zoo@msubaroda.ac.in

Funding information

Department of Biotechnology, Grant/Award
Number: BT/PR11467/MED/31/270/2014

Abstract

Exposure to chlorpyrifos-cypermethrin combination during early development resulted in defective looping and ventricular noncompaction of heart in domestic chicken. The study was extended to elucidate the molecular basis of this novel observation. The primary culture of chicken embryonic heart cells showed a concentration-dependent loss of viability when challenged with this combination of technical-grade insecticides. Comet assay, DNA ladder assay, and analyses of appropriate markers at transcript and protein levels, revealed that chlorpyrifos-cypermethrin combination induced cell death by activating apoptosis. Parallely, the tissues derived from control and experimental group hearts were checked for apoptotic markers, and the result was much similar to that of the in-vitro study. Further analysis showed that chlorpyrifos-cypermethrin combination deranged the expression pattern of the transcriptional regulators of cardiogenesis, namely TBX20, GATA5, HAND2, and MYOCD. This, together with heightened apoptosis, could well be the reason behind the observed structural anomalies in the heart of chlorpyrifos-cypermethrin poisoned embryos.

KEYWORDS

apoptosis, cardiogenesis, chlorpyrifos, cypermethrin, teratogenicity

1 | INTRODUCTION

Prenatal exposure to environmental chemicals is one of the leading causes of birth defects in humans. About four infants in one thousand live births globally possess malformed organs, resulting from chemical exposures during pregnancy.¹ Moreover, among the affected children, over a hundred thousand die every year from malformations and functional irregularities of heart worldwide.² It has been reported that newborns with congenital heart defects (CHD) represent a sizable portion of patients who are diagnosed with pediatric cardiovascular disease.³ Interestingly, epidemiological evidence links maternal occupational exposure to agrochemicals as one of the leading reasons for CHD in infants.⁴ In India, the preferred agrochemical to combat the

insect pests of major crops is a combination of chlorpyrifos (CP) and cypermethrin (CM).⁵ If used in combination, both the chemicals cause a synergistic toxic effect, eventually eliminating all the pest species, which otherwise are resilient to them, when used singularly.⁶ Therefore, it was thought pertinent to evaluate the risk of chlorpyrifos-cypermethrin (CP-CM) combination for their potential to induce CHD.

It is well perceived that CP exerts its toxicity by phosphorylating Acetylcholinesterase, a key enzyme involved in the termination of neuronal stimulus, whereas CM acts by disrupting the neuronal membrane potential.⁷ However, when used in combination, the organophosphate inhibits enzymes involved in the detoxification of pyrethroids, leading to a greater than additive toxicity.⁸ A report from Taiwan suggests invasive toxic effects of CP and CM in young



Chick embryonic cells as a source for generating in vitro model of muscle cell dystrophy

Verma Urja¹ · Kashmira Khaire¹ · Suresh Balakrishnan¹ · Gowri Kumari Uggini¹

Received: 4 July 2018 / Accepted: 19 September 2018 / Published online: 9 October 2018 / Editor: Tetsuji Okamoto
© The Society for In Vitro Biology 2018

Abstract

Chick embryonic cells can be used to develop an easy and economical in vitro model for conducting studies on the disease muscle dystrophy (MD). For this, the limb myoblasts from 11th day chick embryo were isolated and cultured. To this muscle cell culture, anti-dystroglycan antibody (IIH6) was added so as to target the α -dystroglycan and disrupt the connection between the cytoskeletal proteins and the extracellular matrix (which is a characteristic feature of MD). Cells were allowed to differentiate further and the morphometrics and mRNA expression were studied. The IIH6-treated muscle cells displayed changes in morphometry, contractibility, and also atrophy was observed when compared to the control cultures. Concomitant gene expression studies showed an upregulation in TGF- β expression, while the muscle sculpture genes MYOD1, MYF5, LAMA2 and MYOG were downregulated resembling the MD in vivo. This simple and cost-effective method can be useful in studies to further understand the disease mechanism and also in conducting initial studies on effect of novel pharmacological agents.

Keywords Chick embryo · Embryonic cells · Muscle dystrophy · In vitro model · α -dystroglycan

Introduction

The molecular players in development of vertebrate muscles are being studied since late 1980s. Myoblast determination protein 1 (MYOD1), myogenin (MYOG), myogenic factor 5 (MYF5) and Myogenic regulatory factor 4 (MRF4) are the earliest identified myogenic regulatory factors (Davis et al. 1987; Wright et al. 1989; Braun et al. 1989). The complete faction of factors leading to development of muscles during the embryonic development and maintenance as well as regeneration in case of post-embryonic development is still being researched. Ample evidence exist to suggest the fact that myogenesis is a conserved process in evolution, and all the vertebrates bear more or less similar structures and proteins at the muscle tissue level (Braun et al. 1989). Vertebrate sarcolemma contains an assembly of glycoproteins which include α and β sub types of dystroglycan and α , β and γ sub types of sarcoglycan and dystrophin. The components of this complex when isolated and identified were found to be associated with dystrophin protein and

thus widely known as dystrophin-glycoprotein complex (Campbell and Kahl 1989). Any genetic modification leading to defect in gene expression or protein synthesis of any of the proteins of this complex leads to severe muscle developmental defects. Muscular dystrophy (MD) is one such disease leading to progressive muscle weakness and atrophy. Out of many variants of MDs, Duchenne muscular dystrophy (DMD) is the most commonly occurring (Emery et al. 2015; Theadom et al. 2014). It occurs due to a deletion, insertion, point mutation, duplication or similar genetic mutations in dystrophin gene (McGreevy et al. 2015).

The dystrophin and associated proteins provide mechanical strength to contracting muscles. They bind to cytoskeletal components of muscles and also help in signal transduction over muscle membranes. Any deviation from normal genetic structure of these proteins leads to an altered and/or defective gene expression and protein production. The resulting myofibres possess less strength and contractibility as well as regenerative capacity. Till date, an effective cure for MD is not known. The drugs are mainly targeted to the symptoms. Thus, MD remains to be an incurable, grave disorder which leads to the death of many people yearly, worldwide.

Basic biology of MD and clinical aspects of the disease in presence of drugs are studied mostly in mdx mice and cDMD dogs (McGreevy et al. 2015; Manning and

✉ Gowri Kumari Uggini
uggini.gowri-zoo@msubaroda.ac.in

¹ Department of Zoology, Faculty of Science, The Maharaja Sayajirao University of Baroda, Vadodara 390002, India

CERTIFICATE OF PARTICIPATION

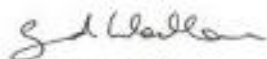
This is to confirm that

Kashmira Khaire

attended the EMBO Workshop

**Molecular mechanisms of developmental and regenerative
biology**

from 11–13 November 2018 in Singapore



Gerind Wallon, PhD
EMBO Deputy Director

**European Molecular
Biology Organization**

Meyerohofstr. 1
69117 Heidelberg
Germany

phone +49 6221 8891 0
fax +49 6221 8891 200

embo@embo.org
www.embo.org

Date and location: 18 November 2018, Heidelberg



International Conference on
Trends in BIOCHEMICAL & BIOMEDICAL Research
Advances and Challenges (TBBR-2018)



Organized by
Department of Biochemistry, Institute of Science
Banaras Hindu University, Varanasi, INDIA

February 13-15, 2018

Certificate

This is to certify that Prof./Dr./Mrs./Mr./Ms. *Kashmira Khairu*
has participated in the International Conference as ~~Chairperson/Invited Speaker/Oral Presenter/Poster~~
~~Presenter/Delegate/Rapporteur/Member of the Organizing Committee/Volunteer.~~
He/She has ~~delivered a lecture/presented scientific paper~~ entitled *Expression profiles of immuno-mod-*
ulators during the wound healing phase of lizard tail regeneration.

P. K. Srivastava
Prof. Pramod K. Srivastava
Convener

Dr. Subash C. Gupta
Dr. Subash C. Gupta
Organizing Secretary